Yield Model of High Fluidity Concrete in Fresh State

Zhuguo Li[1]; Taka-aki Ohkubo[2]; and Yasuo Tanigawa[3]

Abstract: This paper presents a microscopic approach to model the yield condition of high fluidity concrete in the fresh state for the rheological evaluation and the numerical flow simulation to optimize its workability and composition. Based on considering fresh concrete as a type of particle assembly containing water, cohesive particles (cement grains), and cohesionless particles (aggregate grains), the directions and magnitudes of inter-particle forces are examined, the shear deformation resistance of fresh concrete is investigated. Then, an equation of yield condition is derived, and a yield model is proposed for high fluidity concrete in fresh concrete. Furthermore, the dependence of the yield stress on interparticle friction, temperature, normal stress on the shear plane, etc., is clarified on the basis of the obtained yield condition equation.

DOI: 10.1061/(ASCE)0899-1561(2004)16:3(195)

CE Database subject headings: Concrete; Yield stress; Friction; Temperature.

Introduction

High fluidity concrete that can be well cast without compaction has been expected to contribute to rationalization of construction systems and improvement of hardened concrete quality. To achieve self compaction, the appropriate workability is required that is suitable for the position, the geometry, and the reinforcing bar content of the cast structural element, the transportation method, etc. Selecting workability of fresh concrete appropriate to the construction conditions and quality requirements by analytical prediction of the flow behavior is called workability design of concrete (Tanigawa and Mori 1988). Modeling the flow behavior and establishing properly rheological constants for fresh concrete are two of basic works for developing workability design of fresh concrete (Mori 1998).

As the limit stress of the shear flow, yield stress is an indispensable rheological constant that characterizes the flow behavior of high fluidity concrete (Mori 1998). At present, the measurement of yield stress by either the slump test (Komura et al. 1994) or the two-point workability test (e.g., Tattersall and Banfill 1983; Banfill 1990; Wallevik and Gjørv 1990; Hu and Larrad 1996), is actually for Bingham yield stress rather than the true yield stress. The latter is the shear stress at the starting point of the flow curve according to the rheological definition, but the test result of yield stress by the methods mentioned above is an intercept of a near line of measured flow curve on shear stress axis. A lot of experimental studies have reported on the relationship between the constituent and the Bingham yield stress (e.g., Tattersall and Banfill 1983; Hu and Larrad 1996; JCI 1996; Domone et al. 1999), and the effect of normal stress on the shear plane (Mori et al. 1991). However, the research report on the true yield stress has not been found, and modeling of the yield condition has not yet been achieved.

In this study, a microscopic approach is taken for determining the yield stress of high fluidity concrete in a fresh state. After the shear stress supported by fresh concrete is investigated through examining the balance of the resultant of various interparticle forces against the external force considering fresh concrete as a kind of particle assembly, an equation of yield condition of high fluidity concrete in a fresh state is deduced. Based on the obtained yield condition equation, the dependence of the true yield stress on interparticle friction, temperature, and normal stress on the shear plane is clarified, and a yield model is proposed for high fluidity concrete in a fresh state.

Analytical Investigation

Particle Fabric of Fresh Concrete

Fresh concrete composed of water, cement, and aggregates particles, can be regarded as a type of particle assembly, in which the particles have irregular shape and size, and the pore spaces are filled with the water. If we disregard the stress supported by the viscous resistance of the water, the effective stress acting on the skeleton of the particle assembly, i.e., the solid particles, is equal to the applied external static stress. The plane acted on by the maximum shear stress (MS) plane is employed as a reference plane to evaluate the mechanical behaviors of the particles. The normal stress and the shear stress acting on the MS plane are expressed as σ_n and τ, respectively.

Most particles in a particle assembly make contact with surrounding particles. Even those that are suspended completely in the mixing water in the initial state push aside the surrounding water and make contact with others when they move. It is assumed that each particle makes contact with the others only at one point on a certain MS plane (e.g., A and C particles in Fig. 1). If

[1]Domestic Research Fellow, Dept. of Building Materials and Components, Building Research Institute, 1-Tachihara, Tsukuba, Ibaraki 305-0802, Japan.

[2]Chief Research Engineer, Dept. of Building Materials and Components, Building Research Institute, 1-Tachihara, Tsukuba, Ibaraki 305-0802, Japan.

[3]Professor, Division of Environmental Engineering and Architecture, Graduate School of Environmental Studies, Nagoya Univ., Chikusa-ku, Nagoya 464-8603, Japan.

Note. Associate Editor: Jason Weiss. Discussion open until November 1, 2004. Separate discussions must be submitted for individual papers. To extend the closing date by one month, a written request must be filed with the ASCE Managing Editor. The manuscript for this paper was submitted for review and possible publication on November 6, 2002; approved on March 25, 2003. This paper is part of the ***Journal of Materials in Civil Engineering***, Vol. 16, No. 3, June 1, 2004. ©ASCE, ISSN 0899-1561/2004/3-195–201/$18.00.

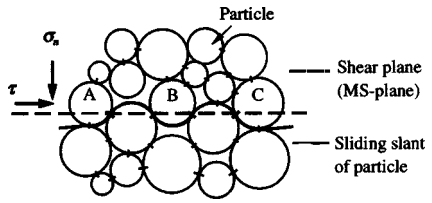

Fig. 1. Particle contact points on maximum shear stress plane

there is more than one contact point (e.g., B particle in Fig. 1), an imaginary one is used to integrate all of them. As a result, the number of contact points is equal to the number of particles on the same MS plane. The number of contact points on a unit dimension of MS plane is expressed as N here.

As shown in Fig. 1, the contact slant or the sliding slant of particles is not generally parallel to the MS plane and changes with their movements. The angle between the particle contact slant and the MS plane direction is called particle contact angle (θ_i). θ_i varies with the particle's position, the surface shape of adjacent particles, etc. It is assumed that θ_i has a normal distribution, and the mean value is noted by θ_m (Fig. 2).

The interparticle friction, which results from the contact between the particles, is thought to be in conformity with Coulomb's friction law. It is also assumed that interparticle friction angle (ϕ_i) has a normal distribution (Fig. 2), where the mean value ϕ_m is a constant for a given fresh concrete specimen. The fabric of particle assembly can be characterized by the distribution form and the mean value of ($\theta_i + \phi_i$) (Murayama 1990), which is called sliding resistance angle of particle in this study. When the particle assembly is loaded, some of the particles move to new stable positions having a larger sliding resistance angle of particle to balance the rising interparticle force caused by the external force. Hence, the particle fabric changes with applied external stress, and θ_m of the particle assembly increases with the applied shear stress (Murayama 1990).

Interparticle Forces

Due to the surface tension and suction of pore water, there is a kind of linking force between the particles, which is perpendicular to the contact plane of particle (Fig. 3). This linking force (f_{wi}) depends on the particle size (r_i), the contact angle (φ_i) of water membrane, and the curvature radii (r_1, r_2), and is given by Eq. (1) for two equisize spheres (Shimada et al. 1993)

$$f_{wi} = f_{ws} + f_{wt} = \pi r_2^2 S_u + 2\pi r_2 \Gamma = \frac{2\pi r_i \Gamma}{1 + \tan(\varphi_i/2)} \tag{1}$$

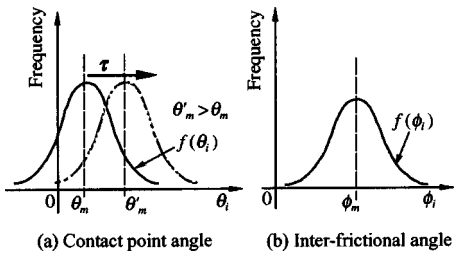

Fig. 2. Distributions of contact point angle of particle and interfrictional angle of particle

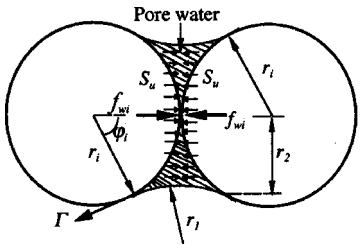

Fig. 3. Interparticle linking force caused by surface tension and suction of pore water

where f_{ws} and f_{wt} = component of linking force portion caused by the suction (S_u) and the surface tension (Γ) of the pore water, respectively.

Only in calculating the interparticle linking force caused by the mixing water by using Eq. (1), do we consider the particles in fresh concrete as spherical bodies with a mean radius, the mean linking force (f_{wm}) resulting from the mixing water is expressed approximately by

$$f_{wm} = \frac{2\pi r_m \Gamma}{1 + \tan(\varphi_m/2)} \tag{2}$$

where r_m = mean size of the particles in fresh concrete; and φ_m = mean water membrane angle.

The surface tension of water is 7.306 Pa at 20°C, and decreases linearly with temperature as shown in the Ramsay–Shield's empirical equation (Watanabe et al. 1973)

$$\Gamma = \alpha \left(\frac{\rho}{M}\right)^{2/3} (T_c - T - 6) \tag{3}$$

where T = temperature; T_c = critical temperature of water; α = constant; ρ = density of water; and M = molecular weight of water.

As well as van der Waals attraction, the cement particles in fresh concrete are also subjected to a static electric repulsion when naphthalene sulfonate-based superplasticizer is added, or to a steric hindrance when polycarboxylate-based superplasticizer is included in the mix (Sakai and Daimon 1996; Uchikawa et al. 1997). The total potential energy formed by these interactions varies with interparticle distance, and hinders the movement of the cement particle. It is considered that stationary cement particles are approximately in equilibrium with the attractive forces and the repulsive forces from surrounding cement particles, so they are subjected only to the interfrictional resistance. However, when cement particles move, they also meet other type of resistance (hereafter referred to as viscous resistance) from the surrounding cement particles due to the breakdown of the attraction–repulsion equilibrium. Murayama (1990) held an investigation on the occurrence mechanism of the viscous resistance of interparticle based on adhesion theory and Eyring's rate process-based viscosity theory. It was concluded that the shear force acting on a particle first destroys the combinations of atom or molecule on the interfaces between the particles, which contribute the solid friction of the interparticle. Only when the particle is moving relatively to its neighboring particles after the combinations were broken does the viscous resistance result from the interparticle potential energy. That is to say, only a motional cement particle is subjected to the viscous resistance in fresh concrete. The viscous interaction force (f_{ei}) between the cement particles caused by this viscous resistance is in the opposite direction from the particle movement.

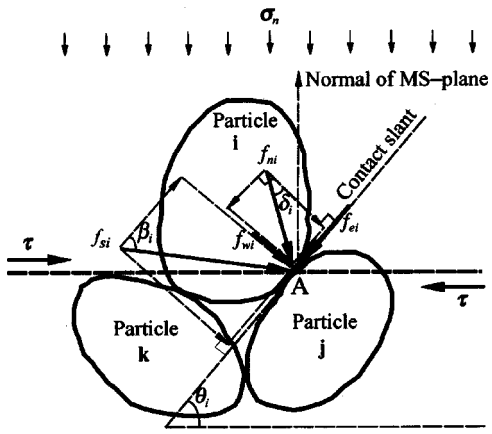

Fig. 4. Interparticle forces and directions

As shown in Fig. 4, when the particle assembly is loaded, any particle i on the MS plane bears the interparticle forces f_{ni} and f_{si} (the resultant is f_i as shown in Fig. 5) from the above and the left particles, respectively. Since the particle i is supported by adjacent particle j at contact point A, it is thought that these interparticle forces (f_{ni}, f_{si}) act on the contact point A. The vector sum of the interparticle forces acting on N contact points on the MS plane should correspond to the shear stresses on the MS plane with respect to either magnitude or direction (Fig. 5). The mean values (f_n, f_s) of f_{ni}, f_{si}, and the mean directional angle (δ_m, β_m) of f_{ni}, f_{si} shown in Fig. 4, are given by

$$f_n=\frac{1}{N}\sum_{i=1}^{N}\{f_{ni}\cos(\hat{f_{ni}\sigma_n})\}=\frac{\sigma_n}{N}$$

$$f_s=\frac{1}{N}\sum_{i=1}^{N}\{f_{si}\cos(\hat{f_{si}\tau})\}=\frac{\tau}{N}$$

$$\delta_m=\frac{1}{N}\sum_{i=1}^{N}\delta_i=\theta_m,\quad \beta_m=\frac{1}{N}\sum_{i=1}^{N}\beta_i=\theta_{\mathbf{m}} \tag{4}$$

where $(\hat{f_{ni}\sigma_n})$ = angle between the direction of f_{ni} and the normal of the MS plane; $(\hat{f_{si}\tau})$ = angle between the directions of f_{si} and the MS plane; β_i = directional angle of f_{si}, which is referred to as the angle between the direction of f_{si} and the contact slant; and δ_i = directional angle of f_{ni}, which is the angle between the direction of f_{ni} and the normal of the contact slant.

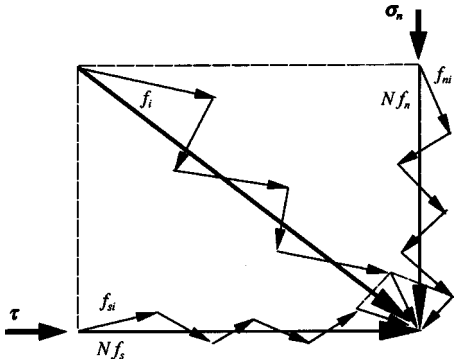

Fig. 5. Mean value of interparticle force f_{si}, f_{ni} caused by external force

Shear Deformation Resistance of Fresh Concrete

If the inertial force of moving particle is ignored, an equilibrium condition in the direction of the contact slant, of the interparticle forces acting on the contact point A, is expressed by

$$f_{si}\cos\beta_i=(f_{si}\sin\beta_i+f_{ni}\cos\delta_i+f_{wi})\tan\phi_i+f_{ni}\sin\delta_i+f_{ei} \tag{5}$$

where f_{ei} = viscous interaction force caused by the potential energy of particle, $f_{ei}=0$ for an aggregate particle or a stationary cement particle; but $f_{ei}\neq 0$ for a moving cement particle.

Since N particles on a unit dimension of the MS plane are all in the mechanical balance state given by Eq. (5), by accumulating the equilibrium equations of N particles, Eq. (6) can be obtained and transformed into Eq. (7)

$$\sum_{i=1}^{N}f_{si}\cos\beta_i=\sum_{i=1}^{N}(f_{si}\sin\beta_i+f_{ni}\cos\delta_i+f_{wi})\tan\phi_i+\sum_{i=1}^{N}f_{ni}\sin\delta_i+\sum_{i=1}^{K}f_{ei} \tag{6}$$

where K = number of moving cement particles.

$$N\left[\frac{1}{N}\sum_{i=1}^{N}f_{si}\cos\beta_i\right]=N\left[\frac{1}{N}\sum_{i=1}^{N}f_{si}\sin\beta_i+f_{ni}\cos\delta_i+f_{wi}\right)\tan\phi_i+N\left[\frac{1}{N}\sum_{i=1}^{N}f_{ni}\sin\delta_i\right]+\sum_{i=1}^{K}f_{ei} \tag{7}$$

The mean value of the product of independent variables is equal to the product of the mean value of each variable (Satou 1961). There is no correlation between f_{ni}, f_{si}, f_{wi}, δ_i, β_i, and ϕ_i. Hence, Eq. (8) can be obtained from Eq. (7) as

$$Nf_s\cos\beta_m=N(f_s\sin\beta_m+f_n\cos\delta_m+f_{wm})\tan\phi_m+Nf_n\sin\delta_m+Kf_{em} \tag{8}$$

and Eq. (9) is obtained by substituting Eq. (4) into Eq. (8)

$$\tau\cos\theta_m=\sigma_n(\cos\theta_m\tan\phi_m+\sin\theta_m)+\tau\sin\theta_m\tan\phi_m+Nf_{wm}\tan\phi_m+Kf_{em} \tag{9}$$

where f_{em} = mean value of f_{ei} of K moving cement particles.

If both sides of Eq. (9) are simultaneously divided by b [$=\cos\theta_m(1-\tan\theta_m\tan\phi_m)$], Eq. (10) is obtained as

$$\tau=\sigma_n\tan(\theta_m+\phi_m)+\frac{1}{b}Nf_{wm}\tan\phi_m+\frac{1}{b}Kf_{em} \tag{10}$$

Eq. (10) shows the shear stress supported by fresh concrete by way of its shear deformation resistance. The shear deformation resistance of fresh concrete is composed of the interfrictional resistance, the resistance resulting from the mean contact angle of particle θ_m (hereafter referred to as fabric-caused resistance), and the viscous resistance of motional cement particles.

Yield Stress and Yield Model of High Fluidity Concrete in Fresh State

There is no potential energy between sand or gravel grains. The sand or gravel grains can turn into the motional state provided the interparticle friction is overcome, thus the deformation of sand or gravel particle group is time independent. However, the cement particle moves relatively to its neighboring particles only when

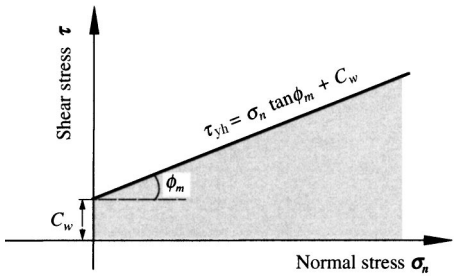

Fig. 6. Shear stress on yield limit of high fluidity concrete in fresh state

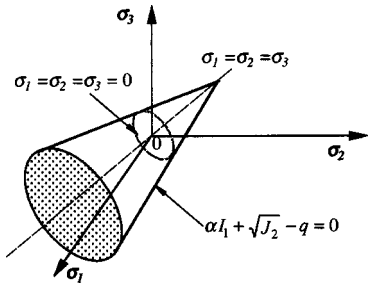

Fig. 7. Yield condition of high fluidity concrete in fresh state

the interfrictional resistance and the viscous resistance caused by the interparticle potential energy are both surmounted by its activation energy being the sum of Brown motion energy and that from applied external force. According to Eyring's rate process-based viscosity theory (Goto 1963), the occurrence of motional cement particle is expressed by a probability, and the number of motional cement particles varies with time. Thus, the movement or deformation of the cement particle group is time dependent. That is to say, when acted on by a shear stress, the aggregate particle group creates an instantaneous deformation, but the cement particle group contributes a delayed deformation. The shear rate is observed only when there are motional cement particles in fresh concrete.

According to the rheology definition, yield stress (τ_y) of high fluidity concrete in the fresh concrete is a limit shear stress, above which the shear deformation rate can be measured. That is to say, motional cement particle is in the absence before fresh concrete yields, τ_y is a sum of the interfrictional resistance and the fabric-caused resistance in the freshly mixed high fluidity concrete, the viscous resistance generated between motional cement particles should not be included. Therefore, by making parameter K in Eq. (10) zero, the yield stress (τ_y) of high fluidity fresh concrete is expressed by

$$\tau_y = \sigma_n \tan(\theta_{my} + \phi_m) + \frac{1}{b} N f_{wm} \tan\phi_m \tag{11}$$

where θ_{my} = mean contact angle of particle of the particle assembly when yield occurs. If the movement of aggregate particles before yielded is ignored, θ_{my} is dependent on the initial particle fabric formed by its own weight of fresh concrete, and, perhaps, compaction.

As stated above, fresh concrete at a rest state supports external force by its shear deformation resistance including the interfrictional resistance and the fabric-caused resistance. High fluidity concrete in the fresh state can flow by its gravity as a suspension. This means that the total inter-resistance of freshly mixed high fluidity concrete is very small. Therefore, it can be considered that its mean particle contact angle (θ_m) approaches zero. Therefore, the yield stress (τ_{yh}) of high fluidity concrete in fresh state can be expressed approximately by

$$\tau_{yh} = \sigma_n \tan\phi_m + N f_{wm} \tan\phi_m = \sigma_n \tan\phi_m + C_w \tag{12}$$

where $C_w = N f_{wm} \tan\phi_m$

Eq. (12) shows that the yield stress of high fluidity concrete in fresh concrete is dependent on its composition through the mean interfrictional angle ϕ_m, and is affected greatly by the normal stress (σ_n) on the shear plane, increases with increasing σ_n for a given specimen.

Substituting Eqs. (2) and (3) into the first equation in Eq. (12), Eq. (13) is obtained as

$$\tau_{yh} = \sigma_n \tan\phi_m + \frac{2\pi N r_m \alpha (\rho/M)^{2/3} (T_c - T - 6)}{[1 + \tan(\varphi_m/2)]} \cdot \tan\phi_m \tag{13}$$

Temperature parameter (T) is included in Eq. (13), and the mean interfrictional angle ϕ_m of granular material varies with environmental temperature (Murayama 1990). Thus the temperature during testing has an effect on the test result of τ_y. If the effect of temperature on ϕ_m is ignored because it is not yet quantitatively clarified, measured yield stress decreases linearly with raising temperature during testing.

Moreover, Eq. (12) has the same form as the Mohr–Coulomb equation, which is generally used to express the shear failure condition of continuous material, rock, and soil. This yield condition, of high fluidity concrete in fresh concrete is illustrated in Fig. 6. Once applied shear stress exceeds the shaded part in this figure, high fluidity concrete will be yielded.

Based on Eq. (12), the yield condition of high fluidity concrete in any stress state can be described by Eq. (14) or by a cone-shaped surface shown in Fig. 7

Table 1. Raw Materials Used and Mix Proportions of High Fluidity Cementitious Materials

Raw materials used		Mix proportions		
		Cement paste	Mortar	Concrete
Mixing water W (kg/m^3)	Potable water	582.9	318.4	212.0
Binder material C (kg/m^3)	Ordinary Portland cement	1,295.3	706.6	471.0
Fine aggregate S (kg/m^3)	Silica sand, diameter: 0.1–0.5 mm	0	1,161	772.6
Coarse aggregate G (kg/m^3)	Glass ball, diameter: 5:7:10 mm = 1:0.6:0.3	0	0	944.4
Admixture AE ($C\times\%$)	Polycarboxylate-based superplasticizer	0	1.5	1.8

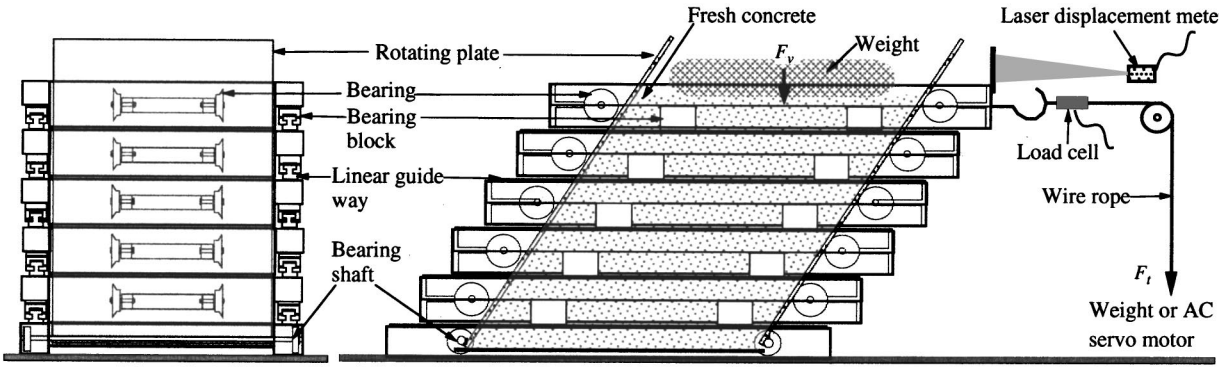

Fig. 8. Shear box apparatus

$$\alpha I_1 + \sqrt{J_2} - q = 0$$

$$\alpha = \tan\phi_m / \sqrt{9 + 12\tan^2\phi_m}$$

$$q = 3C_w / \sqrt{9 + 12\tan^2\phi_m} \tag{14}$$

where I_1 = first invariant of stress; and J_2 = second invariant of stress deviation.

Experimental Investigation

Specimens and Test Procedure of Yield Stress

Materials used and mix proportions of the high fluidity cement paste, mortar, and concrete specimen, are shown in Table 1. Silica sand and glass balls were used respectively as fine aggregate and coarse aggregate for avoiding bad effects of aggregate quality fluctuation on the test result. The cement paste, mortar, or concrete used has a high fluidity, but for avoiding that the fluidity of the mortar or the cement paste is too high to result in segregation during testing, the superplasticizer is not used in cement paste, and the dosage of superplasticizer in mortar is less than that in concrete.

The relationships between the shear strain (γ) of the tested specimen (size: $L18\times W10\times H10$ cm) and load duration (t), are measured with the shear box apparatus shown in Fig. 8 under a series of progressive shear loads from zero (Fig. 9). Then, the shear rates are calculated, which resulted at 10 ms after each shear stress was applied, and the relationship between the shear stress and the resulting shear rate, i.e., a flow curve of the tested specimen is plotted. A stress at the intersection of the flow curve with the shear stress axis is taken as the yield stress of the tested specimen.

Since the maximum shear plane in the specimen is horizontal in this case, the magnitude of normal stress acting on the horizontal shear plane is different from the position of the horizontal shear plane. Thus the shear rate changes along the height direction of the specimen even to a given shear stress. Measured shear rate should be considered to be a mean value of the shear rates on all the horizontal shear planes, which is equivalent to the shear rate under a mean normal stress (σ_{nm}) shown in Eq. (14)

$$\sigma_{nm} = 55.6F_v + \tfrac{1}{2}\rho_c g H \tag{15}$$

where F_v = vertical pressure of the weight on the top surface of specimen (N); ρ_c = unit mass of specimen (kg/m^3); g = gravity acceleration (=9.8 m s^{-2}); and H = height of the specimen (m).

By changing temperature and the weight, respectively, on the top surface of the high fluidity concrete specimen, the yield stresses were measured under different temperatures or mean normal stresses.

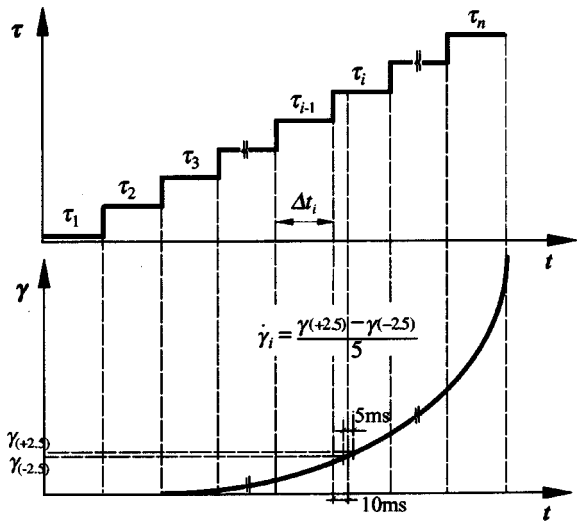

Fig. 9. Progressive shear load and measurement of shear rate

Test Results and Discussion

Fig. 10 show the test results of flow curve for freshly mixed high fluidity concrete under different environmental temperatures. Based on this figure, the yield stresses under different tempera-

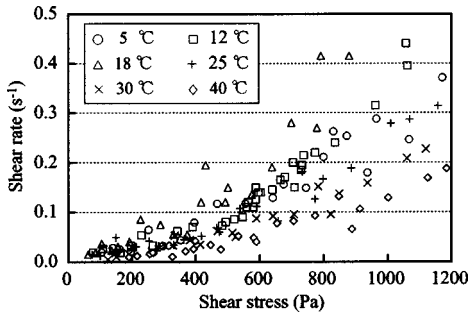

Fig. 10. Effect of temperature on flow curve of high fluidity concrete (σ_{nm} = 1,192 Pa)

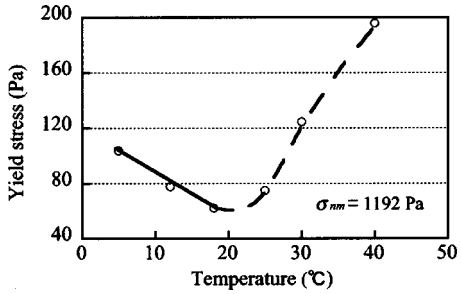

Fig. 11. Variation of yield stress of high fluidity concrete in fresh state with temperature

tures are determined and plotted in Fig. 11, which are the stresses at the intersections of the downward extensions of the flow curves with the shear stress axis. As shown in Fig. 11, the yield stress of high fluidity concrete in the fresh state decreases with the increase in environmental temperature up to a certain limit, and the relationship between the yield stress and temperature during testing approaches a straight line just as indicated in Eq. (13). However, the yield stress increases with increasing temperature when the temperature is above this limit. This is because with the rise in temperature up to the limit, the hydration of cement speeds up, but the increase in hydration rate is still low. The decrease in the yield stress caused by the decrease in the surface tension of mixing water with temperature is greater than the increase caused by the increase in hydrates with temperature. However, when the temperature is too high, the hydrates of cement increase rapidly, and the larger amount of hydrates raises the interfriction of specimen, thus increasing the yield stress.

Fig. 12 shows test results of the yield stress for three types of high fluidity cementitious materials under different mean normal stresses. This figure indicates that yield stress (τ_{yh}) of high fluidity cementitious materials in the fresh state linearly increases with the increase in mean normal stress σ_{nm} that is caused by the specimen's weight and the vertical pressure on its top surface. The $\tau_{yh}-\sigma_{nm}$ relationship can be expressed approximately with a straight line as shown in Fig. 12. Taking the inclination of the straight line as the tangent value of the interfrictional angle of the specimen according to Eq. (12), the interfrictional angles of the freshly mixed cement paste, mortar, and concrete shown in Table 1 are 0.73, 1.64, and 3.21°, respectively. Moreover, the increases (C_w) in the interfriction caused by the surface tension of mixing water are 12.3, 16.5, and 21.2 Pa, respectively. With the aggregates added to the cement paste, the mixture's interfrictional angle and the C_w increase. That the C_w increases with adding the

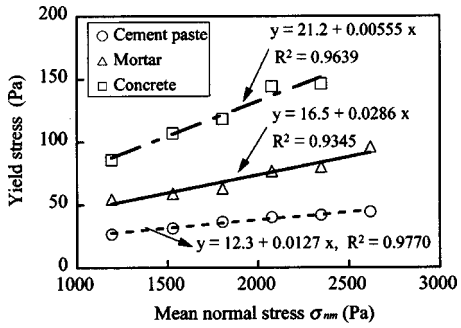

Fig. 12. Effect of normal stress on yield stress of high fluidity cementitious materials in fresh state ($t=12\,°C$)

aggregate is due to the increase in the mean particle radii (r_m) and the decrease in the mean water membrane angle (φ_m) for a certain water content according to Eq. (13). These results indicate that the effect of interfriction on the flow behavior cannot be ignored even for high fluidity cementitious materials. The flow behavior of freshly mixed cementitious materials is dependent on the vertical pressure applied to the shear plane, and this dependence is more remarkable for dry concrete.

Conclusions

The yield behavior of high fluidity concrete in fresh concrete was investigated in this study using a microscopic approach that considers fresh concrete as one kind of particle assembly containing water, cohesive particles (cement grains), and cohesionless particles (aggregate grains). The viscous particle in the motional state also meets the viscous resistance, resulting from the interparticle potential energy, besides the interfrictional resistance and the fabric-caused resistance subjected by the cohesionless particle and stationary viscous particle. The interparticle linking force caused by the surface tension of the mixing water increases the interfriction resistance of fresh concrete. The shear deformation resistance of fresh concrete consists of the interfrictional resistance, the fabric-caused resistance, and the viscous resistance, and is thus dependent on the composition of concrete, pressure on the shear plane, the shear deformation rate, temperature, etc.

The yield stress of high fluidity concrete in the fresh state results from its interfriction. It is therefore dependent on normal stress acting on the shear plane and the surface tension of mixing water. The yield condition of high fluidity concrete in the fresh state shown in Eq. (12) is similar in form to the Mohr–Coulomb equation.

The test result of yield stress of high fluidity concrete in the fresh state increases linearly with the normal stress on the shear plane, but decreases linearly with the rise in environmental temperature within a certain limit.

Notation

The following symbols are used in this paper:

F_t = horizontal pulling force of weight;
F_v = vertical pressure of weight on the top surface of specimen;
f_{em} = viscous interaction force between motional cement particles;
f_{wm} = mean particle-linking force caused by surface tension and section of water;
I_1 = first invariant of stress;
J_2 = second invariant of stress deviation;
K = number of moving cement particles;
N = number of particles in unit dimension particle layer;
r_m = mean radius of particles in fresh concrete;
T = temperature;
Γ = surface tension of mixing water;
τ = shear stress;
τ_y = yield stress of fresh concrete;
τ_{yh} = yield stress of high fluidity concrete;
θ_m = mean contact point angle of particle;
θ_{my} = mean particle contact point angle of fresh concrete when yield occurs;
σ_n = normal stress on the shear plane;

ϕ_m = mean interfrictional angle; and
φ = water membrane angle.

References

Banfill, P. F. G. (1990). ''Use of the ViscoCorder to study the rheology of fresh mortar.'' *Mag. Concrete Res.*, 42(153), 213–221.

Domone, P. L. J., Xu, Y., and Banfill, P. F. G. (1999). ''Developments of the two-point workability test for high-performance concrete.'' *Mag. Concrete Res.*, 51(3), 171–179.

Goto, K. (1963). *Rheology and application*. Kyoritsu Publishing House, Tokyo, 49–51 (in Japanese).

Hu, C., and Larrard, F. D. (1996). ''The rheology of fresh high-performance concrete.'' *Cem. Concr. Res.*, 26(2), 283–294.

Japan Concrete Institute (JCI). (1996). ''Research report on mechanical model of fresh concrete.'' Tokyo, 14–31 (in Japanese).

Komura, R., Tanigawa, Y., Mori, H., and Kurogawa, Y. (1994). ''Rheological study on slumping behavior of fresh concrete.'' *J. Struct. Constru. Eng.*, 462, 1–10 (in Japanese).

Mori, H. (1998). ''High fluidity concrete.'' *J. Archit. Build. Sci.*, 113(1420), 41–43 (in Japanese).

Mori, H., Tanaka, M., and Tanigawa, Y. (1991). ''Experimental study on shear deformational behavior of fresh concrete.'' *J. Struct. Constr. Eng.*, 421, 1–10 (in Japanese).

Murayama, T. (1990). *Theory of mechanical behavior of soil*, Gihodoshuppan Company Limited, Tokyo, 104–107, 273–273 (in Japanese).

Sakai, E., and Daimon, E. (1996). ''The dispersion mechanisms of AE high range water reducing agent.'' *Cem. Concr.*, 595, 13–22 (in Japanese).

Satou, R. (1961). *An introduction to mathematical statistics*, Baifukan Company Limited, Tokyo, 123–123 (in Japanese).

Shimada, K., Fujii, H., and Nishimura, S. (1993). ''Increase of shear strength due to surface tension and suction of pore water in granular material.'' *Proc., Symp. on Mechanical Behaviors of Granular Material, Japan*, 17–20 (in Japanese).

Tanigawa, Y., and Mori, H. (1988). ''Toward the development of workability design of fresh concrete.'' *Cem. Concr.*, 501, 11–20 (in Japanese).

Tattersall, G. H., and Banfill, P. F. G. (1983). *The rheology of fresh concrete*, Pitman Advanced Publishing Program, London, 3–356.

Uchikawa, H., Hanehara, S., and Sawaki, T. (1997). ''Effect of electrostatic and steric repulsive force of organic admixture on the dispersion of cement particles in fresh cement paste.'' *Cement Concrete*, 602, 28–38 (in Japanese).

Wallevik, O. H., and Gjørv, O. E. (1990). ''Modification of the two-point workability apparatus.'' *Mag. Concrete Res.*, 42(152), 135–142.

Watanabe, N., et al. (1973). *Surface and interface*, Kyoritsu Publishing House, Tokyo, 33–36 (in Japanese).